

A molecular basis for NO selectivity in soluble guanylate cyclase

Elizabeth M Boon¹, Shirley H Huang² & Michael A Marletta¹⁻³

Soluble guanylate cyclases (sGCs) function as heme sensors that selectively bind nitric oxide (NO), triggering reactions essential to animal physiology. Recent discoveries place sGCs in the H-NOX family (heme nitric oxide/oxygen-binding domain), which includes bacterial proteins from aerobic and anaerobic organisms. Some H-NOX proteins tightly bind oxygen (O₂), whereas others show no measurable affinity for O₂, providing the basis for selective NO signaling in aerobic cells. Using a series of wild-type and mutant H-NOXs, we established a molecular basis for ligand discrimination. A distal pocket tyrosine is requisite for O₂ binding in the H-NOX family. These data suggest that sGC uses a kinetic selection against O₂; we propose that the O₂ dissociation rate in the absence of this tyrosine is fast and that a stable O₂ complex does not form.

Soluble guanylate cyclase is a heme sensor protein that selectively binds NO at the heme iron, activating the enzyme to convert guanosine triphosphate (GTP) to cyclic guanosine monophosphate (cGMP)¹. cGMP subsequently mediates a number of important physiological processes, including smooth muscle relaxation and neurotransmission. NO, which is present in target cells at a concentration of ~10 nM, is an effective signaling molecule even in the aerobic environment of the cell (intracellular O₂ concentrations are ~20–40 μM) because sGC overcomes the inherent affinity of heme for O₂, thereby preventing a stable iron-oxygen bond and avoiding this highly unfavorable competition. Because the concentration of O₂ is much higher than that of NO in eukaryotic cells, if sGC bound O₂ even weakly, there would be competition for the heme between NO and O₂, resulting in non-selective formation of cGMP, blocking of the specific NO signal, or both. This ability of sGC not to bind O₂ is even more notable in light of the fact that the heme in sGC is identical to that in the O₂ storage and transport globin proteins—that is, they use the same protoporphyrin IX, oxidation state and proximal histidine ligand. The molecular factors that allow sGC to discriminate between the apolar diatomic gases, NO and O₂, are of great interest considering that this discrimination is central to selective biological responses to NO.

The marked selectivity against O₂ exhibited by sGC is highlighted by the discovery of a new family of heme proteins in prokaryotes with substantial homology (15–40% identity) to the heme domain from sGC (Fig. 1)²⁻⁴. Through cloning and initial spectroscopic characterization of several of these sGC-like heme domains, our laboratory found that members of this family from facultative aerobes are spectroscopically similar to sGC, as predicted, forming 5-coordinate NO complexes and rigorously excluding O₂ as a ligand³. The predicted heme sensor domain from the obligate anaerobe *Thermoanaerobacter tengcongensis*, however, is spectroscopically similar to the globins, forming a stable oxygen complex and a 6-coordinate NO complex³.

The family is named the H-NOX domain because spectroscopic results indicate that, using the same protein fold (based on sequence alignment) and an identical heme cofactor, some members of the H-NOX family form a tight complex with O₂ while others, like sGC, can use NO as a ligand by selectively excluding O₂.

We recently reported the structure of the H-NOX domain from the anaerobe *T. tengcongensis* (Tt H-NOX), an O₂-binding member of this family, solved to a resolution of 1.77 Å (ref. 4). One of the prominent features of the O₂-bound structure of the Tt H-NOX domain is the presence of a hydrogen-bonding network around the bound O₂ molecule (Fig. 1). Tyr140 is involved in a 2.74-Å hydrogen bond to the bound O₂, and Asn74 and Trp9 are involved in 2.89-Å and 2.79-Å hydrogen bonds to the phenolic oxygen of Tyr140, respectively. H-NOX sequence alignments show that all three of these residues are found only in anaerobic members of the H-NOX family, which, according to results with Tt H-NOX, are predicted to bind O₂. These residues are absent in all of the H-NOX domains from facultative aerobes and eukaryotes (sGCs) that do not bind O₂ (Fig. 1). Thus, these residues became clear choices for mutagenesis studies aimed at determining the molecular factors involved in ligand discrimination within the H-NOX family. In this report, using the crystal structure as a guide, we examined a series of mutant proteins to develop a structure-function relationship for O₂ binding in the H-NOX family.

RESULTS

The role of a distal tyrosine

Initially, we chose Tt H-NOX Y140L and W9F mutations, as well as the double mutant W9F Y140L, for investigation of their role in O₂ binding to Tt H-NOX. These mutants were generated by standard methods, expressed, purified and spectroscopically characterized as previously reported for wild-type Tt H-NOX³. The structurally conservative Y140F mutant was also generated. Tt Y140F is

¹Department of Chemistry, ²Department of Molecular and Cell Biology, University of California, Berkeley, California 94720, USA. ³Division of Physical Biosciences, Lawrence Berkeley National Lab, Berkeley, California 94720, USA. Correspondence should be addressed to M.M. (marletta@berkeley.edu).

Published online 24 May 2005; doi:10.1038/nchembio704

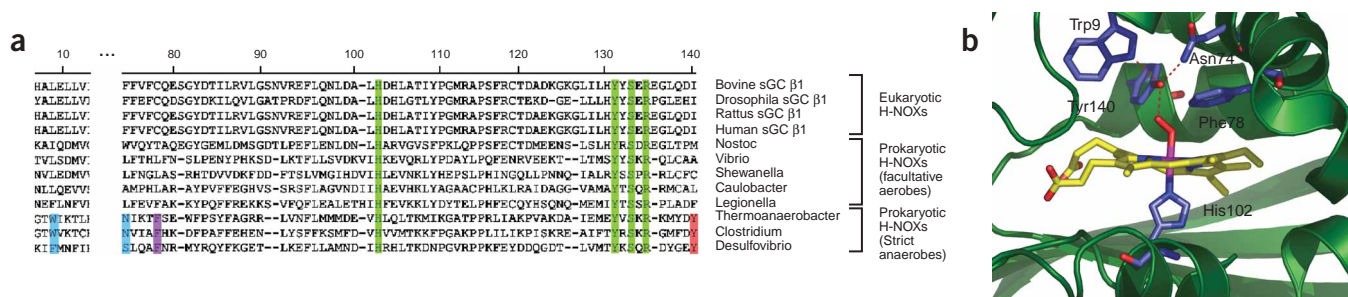


Figure 1 Residues important for ligand discrimination in the H-NOX family. **(a)** Multiple sequence alignment of selected eukaryotic and prokaryotic H-NOX proteins. Numbering corresponds to the Tt H-NOX domain. Residues conserved among all H-NOX proteins are highlighted in green. The O₂-binding Tyr140 from Tt H-NOX is highlighted in red and is conserved among the strict anaerobes. Trp9 and Asn74 and their homologous residues in the other strict anaerobes are highlighted in blue. Phe78, conserved among the strict anaerobes and highlighted in purple, recovers O₂ binding in the Tt H-NOX Y140L F78Y double mutant. Alignments were generated using the program MegAlign. **(b)** Hydrogen-bonding network in Tt H-NOX Fe^{II}-O₂. Tyr140 stabilizing bound O₂ is shown in the crystal structure of Fe^{II}-O₂ Tt H-NOX⁴. Trp9 and Asn74 form a hydrogen-bonding network (red dashes) that directs Tyr140 toward the bound O₂. Phe78 points into the distal pocket and can recover O₂ binding in the Y140L F78Y double mutant. Residues His102 (proximal ligand of the heme Fe^{II}), Tyr140, Trp9, Asn74 and Phe78 are shown in blue. The bound O₂ is shown in red, the heme is shown in yellow (with the Fe^{II} colored pink) and the rest of the protein is colored green.

spectroscopically and kinetically similar to Y140L in the Fe^{II} oxidation state, as described below, but this mutant is very difficult to oxidize; substantial oxidation was achieved only after reaction with 10 mM FeCN₆³⁻ at 42 °C for 1 h, and it formed an Fe^{III}-FeCN₆⁴⁻ complex even after gel filtration. We were unsure if this mutation altered the redox potential of Tt H-NOX or possibly substantially altered the distal pocket such that FeCN₆³⁻ could not easily access the heme, thus we instead pursued Y140L. Leucine is a common distal pocket residue in H-NOX domains as well as other O₂-binding proteins in general.

In the Fe^{II} oxidation state and in buffer saturated with either air or O₂, wild-type Tt H-NOX forms a complex with oxygen with a Soret band at 416 nm and split α/β bands accompanied by an increase in the extinction in the 450- to 500-nm range and resolution of the δ-band, at ~350 nm (Fig. 2a). This complex is stable at temperatures from

0 to 80 °C (70 °C spectrum shown in Fig. 2a), the higher of which is the physiologically relevant temperature for its native organism, *T. tengcongensis*. This spectrum is similar to spectra of the oxy globins. The electronic structure of this complex in Tt H-NOX is probably a resonance structure between Fe^{II}-O₂ and Fe^{III}-O₂⁻ (an {FeO₂}⁸ system). At this time, however, the extent of electron transfer in this protein is unknown, and because a reversible complex forms when O₂ binds to the Fe^{II} form of the protein, the complex is designated Fe^{II}-O₂ for simplicity.

The Tt H-NOX mutant W9F seems also to form an Fe^{II}-O₂ complex, although the Soret maximum shifts to 418 nm (Fig. 2b). Spectroscopic studies of Y140L, however, clearly revealed that the O₂-binding affinity of Y140L is markedly altered (Fig. 2c). Y140L has a Soret maximum of 422 nm and modest splitting of the α/β bands in

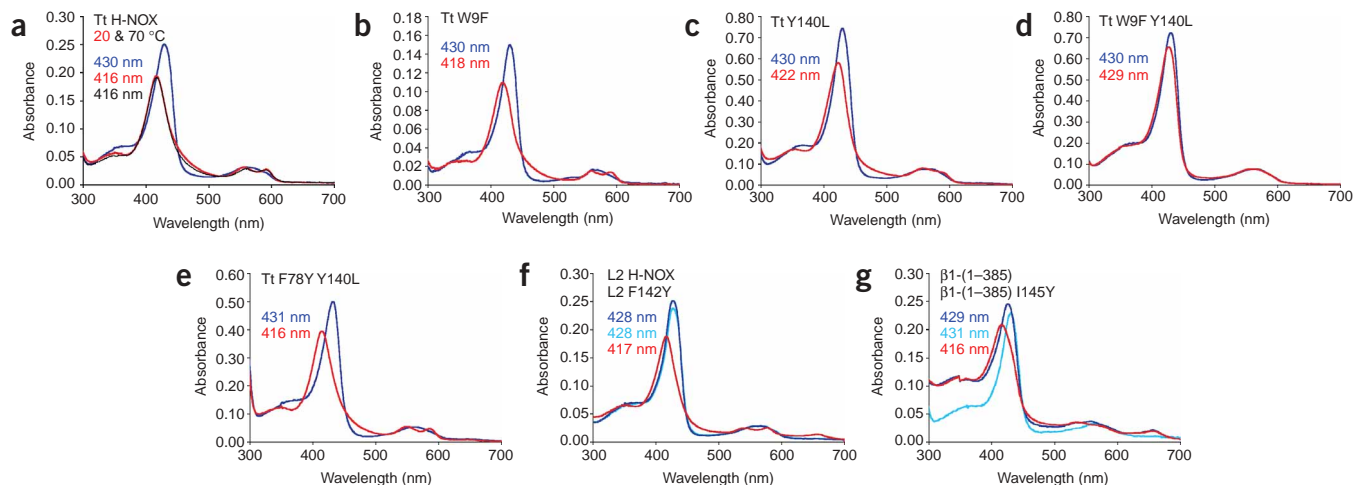
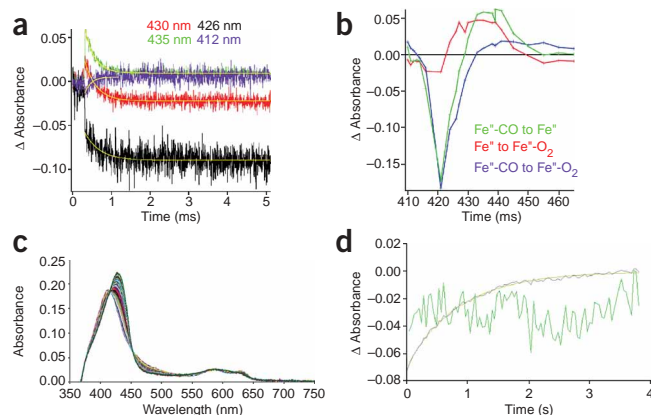


Figure 2 UV-visible spectroscopy of H-NOX proteins after anaerobic reduction (Fe^{II} unligated complexes, blue) before and after being exposed to air (Fe^{II}-O₂ complexes, red). **(a)** Tt H-NOX. **(b)** Tt W9F. **(c)** Tt Y140L. **(d)** Tt W9F Y140L. **(e)** Tt F78Y Y140L. **(f)** L2 H-NOX and L2 F142Y. **(g)** β1-(1-385) and β1-(1-385) I145Y. In addition to the Fe^{II} and Fe^{II}-O₂ complexes of L2 F142Y and β1-(1-385) I145Y, the spectrum of wild-type L2 H-NOX and β1-(1-385) H-NOX after reduction and exposure to air are shown in light blue of **f** and **g** to demonstrate that these proteins do not bind O₂ before the addition of a distal pocket tyrosine. The Fe^{II}-O₂ complex of Tt H-NOX at 70 °C is plotted in black in **a**. These data clearly demonstrate that a tyrosine in the distal heme pocket of the H-NOX heme fold is necessary and sufficient for stabilization of an Fe^{II}-O₂ complex and provide strong indication that one of the keys to ligand discrimination in sGC is the lack of a hydrogen bond donor in the distal pocket.

Figure 3 O₂-binding kinetics of Tt H-NOX. The O₂ association rate (k_{on}) was determined using flash photolysis techniques at 20 °C as described in detail in the text. (a) Transient absorption traces at multiple wavelengths illustrating the decay in absorbance of the Fe^{II} complex due to O₂ association (the single exponential fits are illustrated in yellow). (b) Difference absorption spectra generated from the transient absorption data; these data demonstrate that the transient absorption decay is due to O₂ association. Dissociation rates were measured by stopped-flow spectroscopy at 20 °C. (c) Equal volumes of protein and dithionite were rapidly mixed, and the absorbance spectrum was recorded every 0.002 seconds. (d) The change in absorbance at 437 nm (the wavelength of maximum difference between the Fe^{II} and Fe^{II}-O₂ spectra) was plotted versus time (black) and fit to a single exponential (yellow; residual plotted in green), yielding the rate of O₂ dissociation directly. The kinetic constants for O₂ binding to the other proteins studied in this work were obtained in the same fashion and are reported in **Table 1**.



1 atm of air (258 μ M O₂ dissolved in water), but in 1 atm of O₂ (1.28 mM O₂ dissolved in water), the Soret absorbance is 420 nm with slightly greater splitting of the α/β bands. Notably, we found no evidence for protein oxidation under these conditions using CN⁻ (from KCN) as a spectroscopic probe for Fe^{III}. The best explanation for these results is incomplete O₂ occupation of the heme (that increases with O₂ concentration), consistent with a reduced affinity for O₂, providing the first evidence that Tyr140 is important for stabilization of an Fe^{II}-O₂ complex in the H-NOX family. There seems to be a synergistic effect of mutating both residues, because the W9F Y140L double mutant seems to have lost the capacity for binding oxygen (**Fig. 2d**). Perhaps in the absence of Tyr140, Trp9 can coordinate a water molecule that participates in a weak hydrogen bond with bound O₂, partially stabilizing the complex. This would explain why the double mutant abolishes the ability of Tt H-NOX to bind O₂.

The structure of Tt H-NOX reveals that Phe78 is in the distal pocket, lying just above the heme and pointing toward the bound O₂ (**Fig. 1**). If a distal pocket tyrosine is important for O₂ binding in the H-NOX family, we hypothesized that inclusion of a tyrosine at position 78 may rescue O₂-binding activity in the Y140L mutant. Indeed, spectroscopic characterization of the double mutant F78Y Y140L revealed clearly that it binds O₂ (**Fig. 2e**), indicating that a tyrosine anywhere in the distal pocket that is able to reach an iron-bound O₂ is key in stabilization of an Fe^{II}-O₂ complex.

These mutations revealed the importance of tyrosine for stabilization of O₂ binding in Tt H-NOX. The finding that Tyr140 is found only in the H-NOX domains from members of the family that are predicted to bind O₂ led to the hypothesis that this residue is at the heart of ligand specificity in the H-NOX family of heme domains. To investigate this hypothesis further, we introduced a tyrosine into the homologous position of the distal heme pocket of two H-NOX proteins (both a prokaryotic H-NOX and a eukaryotic sGC H-NOX) that do not bind O₂ (see **Fig. 1a** for homology alignment). We initially chose the H-NOX domain from *Legionella pneumophila* (L2 H-NOX) for site-directed mutagenesis because, like sGC, L2 H-NOX does not bind O₂ (**Fig. 2f**) and it has a phenylalanine at position 142, the homologous position to Tyr140 in Tt H-NOX (**Fig. 1**), making F142Y a structurally conservative mutation. Upon purification and characterization, it was immediately obvious that L2 F142Y was capable of binding O₂ (**Fig. 2f**). L2 F142Y was purified as the Fe^{II}-O₂ complex (Soret maximum at 417 nm) and is spectroscopically more similar to Tt H-NOX than wild-type L2 H-NOX.

This hypothesis was conclusively tested by introduction of a tyrosine side chain into the distal pocket of the heme domain from

the β 1 subunit of rat sGC (β 1-(1-385)). The point mutation, β 1-(1-385) I145Y, resulted in a protein that now binds O₂. Upon reduction and exposure to air or O₂, the Soret maximum shifted from 429 to 416 nm (**Fig. 2g**), consistent with formation of an Fe^{II}-O₂ complex by comparison to Tt H-NOX and the globins. This 416-nm complex is ferrous, as we found no evidence for protein oxidation using CN⁻ (from KCN) as a spectroscopic probe for Fe^{III} and we converted the 416-nm species into an Fe^{II}-CO complex (at 423 nm) by incubation under a CO atmosphere for 20 min. After exposure to O₂, a shoulder on the Soret band at 429 nm remained and there was only modest splitting of the α/β bands even under 1 atm of O₂, indicating the O₂ affinity is low and some Fe^{II} unligated complex remains in solution. Nonetheless, this single mutation in sGC, a protein that has no measurable affinity for O₂, converted it into a protein that does bind O₂. This notable result now provides conclusive evidence that the lack of a distal pocket hydrogen bond donor, a tyrosine in particular, is the primary molecular factor in its discrimination against O₂.

A distal pocket tyrosine affects k_{off}

To quantify the importance of distal pocket hydrogen bonding for O₂ binding within the H-NOX domain, we determined the O₂-binding kinetics of Tt H-NOX, wild type and mutants, as well as L2 F142Y H-NOX and β 1-(1-385) I145Y. The O₂ association rates (k_{on}) were determined using flash photolysis techniques at 20 °C (ref. 5). From equilibrium titration experiments, we knew that the K_d for O₂ binding to Tt H-NOX had to be very low because generation of the Fe^{II} 5-coordinate complex was very difficult to maintain free of O₂, even using anaerobic techniques. Thus, Fe^{II} was generated transiently by flash photolysis of the Fe^{II}-CO complex, which in aerobic solutions is rapidly bound by O₂. This association was monitored by transient absorption spectroscopy. In transient absorption traces of several flash photolysis experiments followed at various wavelengths for the wild-type Tt H-NOX (**Fig. 3a**), the initial spike corresponds to the difference in absorbance between the Fe^{II}-CO complex and the Fe^{II} unligated species, and the decay is due to O₂ binding and thus loss of absorbance of the Fe^{II} complex. The difference between the initial absorbance value before the flash and the absorbance value of the final decay is due to the difference in absorbance of the Fe^{II}-CO and Fe^{II}-O₂ complexes. Using this transient absorption data, the difference absorption spectra were generated for each transition (**Fig. 3b**). These correlate very well with the equilibrium difference spectra (data not shown). The association rate was determined by fitting the absorbance decay to a single exponential (shown in yellow in **Fig. 3a**). This rate was independent of observation wavelength but dependent on O₂ concentration.

Table 1 Kinetics constants for O₂ reactions with some ferrous heme domains

Protein	K_d (nM) ^a	k_{on} ($\mu\text{M}^{-1} \text{s}^{-1}$)	k_{off} (s^{-1})	k_{ox} (h^{-1})	Distal pocket residues	Reference
Sw Mb	880	17	15	0.006	His (E7), Leu (B10)	8
Soybean Leg-Hb	43	130	5.6	0.2	His (E7), Tyr (B10)	25
Mt HbN	8	25	0.2	$t_{1/2} = 537 \text{ h}$	Leu (E7), Tyr (B10)	20
Ascaris Hb	2.7	1.5	0.004		Glu (E7), Tyr (B10)	24
Trematode Hb	0.28	108	0.03		Tyr (E7), Tyr (B10)	26
HemAT-B	720	32	23	0.06	Ser (E7), Leu (B10)	9
Ax PDEA1H	12,000	6.7	77	$t_{1/2} > 12 \text{ h}$	Arg87, Ile82, Leu105	28
Bj FixL	140,000	0.14	20	2.7	Arg220, Ile215, Ile238	27
Tt H-NOX	89.7 ± 6.2	13.6 ± 1.0	1.22 ± 0.09	– ^b	Trp9, Phe78, Tyr140	This work
Tt H-NOX (NO) ^c	ND ^d	ND ^d	$(5.6 \pm 0.5) \times 10^{-4}$		Trp9, Phe78, Tyr140	This work
Tt W9F	305 ± 31	6.02 ± 0.62	1.84 ± 0.17	– ^b	Phe9, Phe78, Tyr140	This work
Tt Y140L	$\sim 1,400$	– ^e	20.1 ± 2.0	0.19	Trp9, Phe78, Leu140	This work
Tt Y140L (NO) ^c	ND ^d	ND ^d	$(1.3 \pm 0.3) \times 10^{-4}$		Trp9, Phe78, Leu140	This work
Tt W9F Y140L	– ^f	– ^f	– ^f	0.12	Phe9, Phe78, Leu140	This work
Tt F78Y Y140L	ND ^d	ND ^d	0.83 ± 0.17	– ^b	Trp9, Tyr78, Leu140	This work
L2 F142Y	$9,200 \pm 3,000$	0.40 ± 0.14	3.68 ± 0.71	– ^g	Phe9, Phe78, Tyr142	This work
$\beta 1(1-385)$ I145Y	$\sim 70,000,000$	$\sim 0.00004^h$	2.69 ± 0.61	0.72	Leu9, Cys78, Tyr145	This work

^aDissociation constants (K_d values) for O₂ binding at 20 °C were determined by the ratio of k_{off}/k_{on} . ^bAutoxidation rates at 37 °C were measured by changes in the UV-visible spectroscopy and recorded as further indication of the ability of distal hydrogen bonds to stabilize the inherent reactivity of Fe^{II}-O₂ complexes. Tt H-NOX and the mutants W9F and F78Y Y140L have extremely slow rates of autoxidation; after >24 h at 37 °C, there was no indication of any oxidation by UV-visible spectroscopy. The autoxidation rates for the Y140L and W9F Y140L mutants, while measurable, are quite slow, comparable with those reported for other O₂-binding heme proteins. ^cNO dissociation rates were measured for Tt H-NOX and Tt Y140L, in addition to the O₂ dissociation rates. Geminate recombination of NO was prevented using a CO/dithionite trap. ^d k_{off} (NO) was measured by monitoring the formation of the Fe^{II}-CO complex at 424 nm over time. ^eND, not determined. ^fWe were unable to determine conclusively k_{on} for the Tt Y140L mutant because of very fast geminate CO recombination kinetics, even in aerobic buffer with no excess CO. Geminate CO recombination kinetics have also been measured in apolar distal pocket mutants of myoglobin¹⁹. Despite being somewhat complicated by geminate CO recombination, the O₂ association rate to Y140F ($k_{on} = 15.7 \pm 1.4 \mu\text{M}^{-1}\text{s}^{-1}$) was obtained. ^gNo O₂ complex formed even in buffer equilibrated with 1 atm pure O₂. ^hL2 F142Y precipitated as it oxidized, making it difficult to measure the k_{ox} . ⁱThe association rate for $\beta 1(1-385)$ I145Y was too slow to measure with transient absorbance techniques. k_{on} was estimated from monitoring the shift in the Soret from 429 nm to 416 nm over time under 1 atm of air (210 μM O₂) at 37 °C.

In general, the distal pocket mutations do not have a large effect on the association rates in Tt H-NOX ($6\text{--}15 \mu\text{M}^{-1}\text{s}^{-1}$). The L2 F142Y and $\beta 1(1-385)$ I145Y mutants are the exception. L2 F142Y has a relatively slow k_{on} of $0.40 \mu\text{M}^{-1}\text{s}^{-1}$ and $\beta 1(1-385)$ I145Y has an extremely slow k_{on} , estimated to be $\sim 0.00004 \mu\text{M}^{-1}\text{s}^{-1}$ from monitoring the shift in the Soret from 429 nm to 416 nm over time under 1 atm of air (258 μM O₂). At room temperature, this process takes > 1 h, but it is faster at 37 °C. These slow association rates may occur because the L2 and $\beta 1$ H-NOX proteins contain only the tyrosine without the rest of the distal pocket hydrogen-bonding network present in Tt H-NOX. The secondary hydrogen bonds from asparagine and tryptophan serve to direct tyrosine toward the iron center, forcing a strong hydrogen bond. The unnatural tyrosine in these mutants may have more conformational flexibility, which effectively slows the process of aligning the O₂ and the tyrosine hydroxyl for a strong and directed hydrogen bond. We suspect that in the $\beta 1(1-385)$ I145Y mutant in particular, the tyrosine might be directed away from the heme in its most stable conformation, and then as protein dynamics transiently brings the tyrosine toward the heme, O₂ is captured, leading to the formation of a stable Fe^{II}-O₂ bond. This hypothesis is consistent with the very slow association rate and the increase in this rate at higher temperatures. This interpretation is supported by the association kinetics of Tt W9F. Loss of Trp9, which provides a hydrogen bond to Tyr140 in Tt H-NOX as a part of the hydrogen-bonding network in the distal pocket, also resulted in slightly reduced O₂ association (two-fold), which could be due to increased movement of Tyr140. Modulation of O₂ affinity has similarly been attributed to the B10 and E11 residues in the globins⁶⁻¹¹.

Dissociation rates were measured by stopped-flow spectroscopy techniques at 20 °C as illustrated for Tt H-NOX in **Figure 3c,d**. The change in absorbance at 437 nm (the wavelength of maximum difference between the Fe^{II} and Fe^{II}-O₂ spectra) was plotted versus time and fit to a single exponential, yielding the rate of O₂ dissociation

directly. The dissociation rates measured are independent of dithionite concentration (100, 50, 25, 10, 5 and 2.5 mM dithionite were tested) and independent of saturating CO as a trap for the reduced species, both with and without 10 mM dithionite present. We obtained the kinetic constants for O₂ binding to the other proteins studied in this work in the same fashion (see **Table 1**).

Comparison of the dissociation rates immediately demonstrates the importance of a distal pocket tyrosine in stabilization of bound O₂ (**Table 1**). Lack of the tyrosine, in Tt Y140L, increases the dissociation rate by 20-fold. The secondary distal pocket hydrogen bonds do not seem to contribute to the dissociation rates as much as they do to the association rates (absence of Trp9 has almost no effect on k_{off}). It seems that once O₂ is bound with a strong and directed hydrogen bond to tyrosine, there is little mobility even without secondary hydrogen bond donors. Most notably, L2 F142Y and $\beta 1(1-385)$ I145Y have very slow dissociation rates, near that of wild-type Tt H-NOX, whereas their wild-type counterparts do not bind O₂ at all. This stabilization is entirely due to the simple replacement of a single residue within the distal pocket, with no additional secondary hydrogen bonds. In fact, in L2 H-NOX this is due only to the replacement of a hydrogen (-H) with a hydroxyl group (-OH). Within the H-NOX fold, this position seems perfectly placed to form an extremely strong and directed hydrogen bond with bound O₂, providing a single-residue switch to either eliminate O₂ binding or strongly stabilize an Fe^{II}-O₂ complex. These data indicate that sGC excludes O₂ as a ligand based on kinetics; the O₂ dissociation rate in the absence of a distal pocket hydrogen bond donor is probably so fast that a stable O₂ complex does not form.

Tyrosine is important for discrimination of O₂ and NO

To provide evidence that the distal pocket tyrosine, in addition to stabilizing the Fe^{II}-O₂ complex, is also playing a role in discrimination

between NO and O₂, we measured the NO dissociation rates for Tt H-NOX and Tt Y140L (**Table 1**). Although we do not have data for the association rates at this time, and thus cannot calculate a K_d for NO binding to these proteins, the dissociation rates indicate that removing the distal pocket hydrogen bond from Tt H-NOX (Tt Y140L), if anything, may result in a more stable NO complex (k_{off} is 5.6 × 10⁻⁴ s⁻¹ and 1.3 × 10⁻⁴ s⁻¹ for Tt H-NOX and Tt Y140L, respectively). These data suggest that a distal pocket hydrogen bond is not required for NO binding by Tt H-NOX. Together with the O₂ kinetic data, it seems that Tt H-NOX has evolved to distinguish NO and O₂ using Tyr140.

DISCUSSION

Nitric oxide is an essential signaling molecule in animal physiology. As the receptor for NO, sGC has evolved to discriminate between NO and O₂, providing for the specific use of NO within aerobic eukaryotic cells. The origin of this selectivity has been an important and open question since the discovery that sGC binds NO with a ferrous histidyl-ligated heme. Previous hypotheses for ligand discrimination in sGC have included (i) a weak Fe-histidine bond, estimated from measurement of the Fe-histidine bond stretch using resonance Raman spectroscopy (RR)¹², which cannot support a strong Fe-O bond¹³; and (ii) negative polarity in the distal heme pocket as indicated by the ν(C-O) stretch in the RR of the Fe^{II}-CO complex^{12,14}. Recent reports from our group on the RR of other prokaryotic members of the H-NOX family that, like sGC, do not bind O₂ but do form 5-coordinate Fe^{II}-NO complexes have ruled out these simple explanations³. One such protein, the H-NOX domain from *Vibrio cholerae*, has an even stronger Fe-histidine bond than Tt H-NOX, as indicated by RR, and all H-NOX domains characterized to date, regardless of O₂-binding capacity, have nearly identical ν(C-O) stretches.

The data presented here outline a new hypothesis for ligand discrimination in the H-NOX family and provide a molecular foundation for selective ligand binding in the control of complex biological responses. We have demonstrated that the presence of a hydrogen-bonding network in the distal pocket of O₂-binding H-NOX proteins is important, and a distal pocket tyrosine, or other residue capable of forming a strong hydrogen bond to bound O₂, is critical. In fact, the mutants Tt F78Y Y140L, L2 F142Y, and in particular, the noteworthy result with β1-(1-385) I145Y now provide conclusive evidence that this tyrosine is necessary and sufficient for O₂ binding. The origin of this selectivity is kinetic; a distal pocket tyrosine markedly slows the dissociation rate for all of Fe^{II}-O₂ complexes in H-NOX domains we have investigated thus far. In fact, it seems that appropriate placement of a tyrosine within the distal pocket of the H-NOX fold acts as a switch for O₂ binding, suggesting that the lack of a distal pocket hydrogen bond in sGC eliminates O₂ as a ligand, making the sGC H-NOX domain selective for NO, and providing for its use as a signaling molecule in an aerobic environment. sGC can effectively use NO as a physiologically important signaling molecule in the aerobic cell, because there are no residues in the distal pocket capable of forming a strong hydrogen bond with heme-bound O₂.

All of the predicted H-NOX domains in strict anaerobes contain a conserved distal pocket tyrosine that aligns with Tyr140 of Tt H-NOX (**Fig. 1a**). Some of the obligate anaerobe H-NOX domains, *Clostridium botulinum* (Cb H-NOX) in particular, also contain conserved counterparts to Trp9 and Asn74. The prediction, then, based on the results reported here, is that these H-NOX proteins will all bind O₂. Because all members of this family that bind O₂ also bind NO, it follows that Cb H-NOX, as well as the rest of the H-NOX domains from strict anaerobes, will also bind both ligands. In contrast to this

prediction, however, it has recently been reported that Cb H-NOX (residues 1-186) does not bind O₂ but binds NO with a femtomolar K_d (NO)¹⁵. Citing this very high affinity for NO, the authors propose that Cb H-NOX probably acts as an NO sensor. These authors did not measure the k_{on} (NO) for this protein but instead assumed it would be diffusion limited as has been reported for sGC¹⁶, and they measured k_{off} (NO) by following the EPR spectrum over time in the absence of a chemical trap for released NO. If the measured dissociation rate is influenced by NO rebinding, as would be expected for a femtomolar NO sensor with a diffusion-limited association rate, then the true dissociation rate is probably faster than reported, and likewise the K_d (NO) is probably higher than reported. In fact, at this time, classification of any of the prokaryotic H-NOX domains as sensors of NO and/or O₂ awaits functional characterization. The nature of the possible differences between Cb H-NOX and Tt H-NOX is not presently clear.

Function of the H-NOX family as heme sensors is a reasonable hypothesis at this time, however, and the results reported here suggest a mechanism of evolution for divergent ligand-binding properties within the H-NOX family. The progenitor H-NOX domain probably appeared first in bacteria, possibly as a stand-alone protein. Over time, in facultative aerobic bacteria, the protein may have evolved to function as a sensing domain, probably for NO derived from NO₃⁻ and signaling a shift to growth in a low-O₂ environment. Many of the facultative aerobic H-NOX domains are in operons with histidine kinases, consistent with a role in signaling. In anaerobic bacteria, such as *T. tengcongensis*, the progenitor H-NOX domain gained distal pocket hydrogen bonds that can stabilize the heme domain as an O₂-binding domain, probably as an O₂ sensor for chemotaxis as these H-NOX domains are fused to methyl-accepting chemotaxis proteins. A role for NO sensing in obligate anaerobes is equally tenable at this point. Possibly through lateral transfer from NO-sensing aerobic bacteria², this domain later appeared in eukaryotes as the sensing domain for guanylate cyclases.

As proposed for H-NOX domains in prokaryotes, within the eukaryotic cyclases, addition of a distal pocket hydrogen bond by a single mutation could lead to O₂-sensitive cyclases. Consistent with this hypothesis, recently we reported an O₂-regulated response in *Caenorhabditis elegans* that requires cGMP and a predicted sGC subunit, whose H-NOX domain binds O₂, suggesting that it is indeed an O₂-sensing sGC¹⁷. Furthermore, recent results suggest there may be O₂-responsive sGCs in *Drosophila melanogaster*¹⁸. Underlying this hypothesis is the fact that the H-NOX family is unique in that it uses the same protein fold either to bind NO and rigorously exclude O₂, or to bind O₂ with very high affinity (**Table 1**), a very difficult task in coordination chemistry. The results reported here, especially the gain of function in L2 H-NOX and β1-(1-385), however, indicate that with engineering of just a few key residues, ligand discrimination is achieved.

This new hypothesis for ligand discrimination in the H-NOX family is consistent with the large body of data available for the globins. Olson and co-workers, over the last 15 years, have extensively mutated the distal pocket of myoglobin and analyzed the structures, spectral characteristics and kinetics of these mutants^{6-8,14,19}. Using these data, they have effectively argued that the key factor for ligand discrimination in favor of O₂ over CO and NO in the globins consists of favorable electrostatic interactions between a polar Fe-O bond (much more polarized than Fe-N or Fe-C in the NO and CO complexes) and the distal pocket His64. A hydrogen bond between His64 and bound O₂ stabilizes the complex by a factor of ~1,000 as compared with the complex without a hydrogen bond, whereas a hydrogen bond with bound CO or NO provides much less stabilization, only a factor of

~2–3 and ~10, respectively, as a result of the less polar nature of the ferrous complexes with those ligands.

It was not initially obvious, however, that the H-NOX family would use some of the same principles as the globins to control O₂ affinity. In fact, as discussed earlier, proposals for ligand discrimination by sGC included proximal heme pocket effects. Furthermore, O₂-binding heme proteins of different folds have adopted different strategies for ligand selectivity. Even within the basic globin fold, differences exist for ligand regulation. Most of the members of the globin family use distal pocket hydrogen bond donors for ligand discrimination; however, hexacoordination has emerged as a new method for ligand discrimination in certain truncated hemoglobins²⁰, nonsymbiotic plant hemoglobins²¹ and neuroglobin²², for example. FixL, which has adopted a PAS fold, also contains a histidine-ligated protoporphyrin IX cofactor for O₂ binding but uses a conformational change of the heme group itself as well as of an arginine-containing loop region in the distal pocket to achieve specific ligand recognition²³. Thus, because the H-NOX family represents a new fold for heme proteins, it was not clear how this new family would achieve ligand selectivity.

Only now is it clear that within the H-NOX fold, distal pocket hydrogen bonding is used to stabilize O₂ as a ligand. More importantly, and what was initially less obvious, is that sGC makes use of the lack of a distal pocket hydrogen-bonding donor to exclude O₂ as a ligand. sGC is required to bind NO in the presence of a much higher concentration of O₂, so it does not use distal pocket hydrogen bonds that selectively stabilize O₂. Tt H-NOX, being an obligate anaerobe, needs to sense O₂ at very low concentrations to avoid entering an aerobic environment; thus the extra stabilization provided by distal pocket hydrogen bonds is used to decrease its K_d for this molecule.

The NO dissociation rates reported here further suggest that a distal pocket hydrogen bond is not required for NO binding by Tt H-NOX. In light of the O₂ kinetic data, which demonstrate that Tyr140 is required for stabilization of an O₂ complex, it seems that Tt H-NOX has evolved to distinguish NO and O₂ using Tyr140. Furthermore, it seems reasonable to extend this conclusion to the H-NOX family as a whole, considering that sGC and all of the other H-NOX family members that do not bind O₂ are predicted to lack distal pocket hydrogen bond donors on the basis of structural alignment with Tt H-NOX.

Our data, as well as those published for myoglobin discussed earlier, suggest that, indeed, distal pocket hydrogen bond donors preferentially stabilize an O₂ complex. Tt Y140L emphasizes this conclusion; removal of the distal pocket hydrogen bond from Tt H-NOX results in an order of magnitude lower affinity for O₂ than wild type but does not have an overall effect on its complex with NO. Therefore, for sGC to function as an NO sensor in an environment of micromolar oxygen concentrations, hydrogen bond donors are omitted from the distal pocket.

The data presented here, in fact, in the context of all of the kinetic data available for various O₂-binding heme proteins (a few examples of which are listed in Table 1) outline a strategy not only for stabilizing O₂ binding but also for tuning O₂-binding affinity based on distal pocket residues. Myoglobin and hemoglobin have distal pocket histidines that stabilize O₂ binding with a K_d in the mid to high nanomolar range⁸. Certain globins, however, such as the truncated globins, have distal pocket tyrosine residues and they have much lower K_d values for O₂, in the nanomolar range^{20,24,25}. The highest known O₂ affinities are in proteins like trematode hemoglobin, which uses two distal pocket tyrosine residues in stabilizing O₂ binding²⁶. The PAS domain O₂-binding heme proteins, however, have mainly hydrophobic distal pocket residues and they have affinity for O₂ in the

micromolar range^{27,28}. Here we have demonstrated that the addition or subtraction of primary and secondary distal hydrogen bonds can tune the affinity of the H-NOX fold from low nanomolar to micromolar (Table 1), and we now have the experimental framework in place to test the effect of other distal pocket hydrogen bond donors, such as histidine, on O₂ affinity in the H-NOX family.

In summary, we have shown that a distal pocket tyrosine is necessary and sufficient for O₂ binding in the H-NOX family. This effect comes primarily from slowing the rate of O₂ dissociation. We have provided conclusive evidence that the remarkable ligand discrimination seen in sGC is due to a very fast O₂ dissociation rate resulting from the lack of a distal pocket tyrosine or alternative hydrogen bond donor. Furthermore, Tt H-NOX uses a network of distal pocket hydrogen bonds, involving Trp9 in addition to Tyr140, that fine-tune the affinity of this protein for O₂. Distal pocket hydrogen bonds and networks seem to be a general strategy for modulating O₂-binding affinity throughout the spectrum of O₂-binding heme proteins, and in the H-NOX family of heme proteins, distal pocket hydrogen bonds are used to carefully engineer ligand specificity, which is necessary for control of selective biological responses.

METHODS

Materials and general methods. Unless otherwise noted, we purchased all reagents in their highest available purity and used them as received.

Protein expression and purification. Cell culture procedures and purification of H-NOX proteins were carried out as described³. Mutagenesis was carried out using the QuikChange protocol from Stratagene.

Electronic spectroscopy. All spectra were recorded on a Cary 3E spectrophotometer equipped with a Neslab RTE-100 constant-temperature bath set to 20 °C. Preparation of complexes was carried out as described³.

O₂ association rate. O₂ association to the heme was measured using flash photolysis at 20 °C. It was not possible to flash off the Fe^{II}-O₂ complex as a result of very fast geminate recombination kinetics; thus the Fe^{II}-CO complex was subjected to flash photolysis with laser light at 560 nm, producing the 5-coordinate Fe^{II} intermediate, to which the binding of molecular O₂ was followed at various wavelengths. Protein samples were made by anaerobic reduction with 10 mM dithionite, followed by desalting on a PD-10 column. This was then diluted to 20 μM heme in 50 mM TEA, 50 mM NaCl, pH 7.5 buffer in a controlled-atmosphere cuvette. CO gas was flowed over the headspace of this cuvette for 10 min to form the Fe^{II}-CO complex, the formation of which was verified by UV-visible spectroscopy (Soret maximum 423 nm). This sample was then either used to measure CO-rebinding kinetics after flash photolysis while still under 1 atm of CO gas, or it was opened and stirred in air for 30 min to fully oxygenate the buffer before flash photolysis to watch O₂-rebinding events. O₂ association to the heme was monitored at multiple wavelengths versus time. These traces were fit with a single exponential using Igor Pro software. This rate was independent of observation wavelength but dependent on O₂ concentration. UV-visible spectroscopy was used throughout to confirm all the complexes and intermediates. Transient absorption data were collected using instruments described²⁹. The instrument possesses a response time of 20 ns, and the data are digitized at 200 megasamples s⁻¹.

O₂ dissociation rate. Fe^{II}-O₂ complexes of protein (5 μM heme), diluted in anaerobic 50 mM TEA, 50 mM NaCl, pH 7.5 buffer, were rapidly mixed with an equal volume of the same buffer (anaerobic) containing various concentrations of dithionite and/or saturating CO gas. Data were acquired on a HI-TECH Scientific SF-61 stopped-flow spectrophotometer equipped with a Neslab RTE-100 constant-temperature bath set to 20 °C. The dissociation of O₂ from the heme was monitored as an increase in the absorbance at 437 nm, a maximum in the Fe^{II} - Fe^{II}-O₂ difference spectrum, or 425 nm, a maximum in the Fe^{II} - Fe^{II}-CO difference spectrum. The final traces were fit to a single exponential. Each experiment was done a minimum of six times, and the

resulting rates were averaged. The dissociation rates measured are independent of dithionite concentration (100, 50, 25, 10, 5 and 2.5 mM dithionite were tested) and independent of saturating CO as a trap for the reduced species, both with and without 10 mM dithionite present.

Rate of autoxidation. Protein samples were anaerobically reduced, then diluted to 5 μM heme in aerobic 50 mM TEA, 50 mM NaCl, pH 7.5 buffer. These samples were then incubated in a Cary 3E spectrophotometer equipped with a Neslab RTE-100 constant-temperature bath set to 37 $^{\circ}\text{C}$ and scanned periodically. The rate of autoxidation was determined from the difference between the maximum and minimum in the $\text{Fe}^{\text{III}} - \text{Fe}^{\text{II}}$ difference spectrum plotted versus time and fit with a single exponential.

NO dissociation rate. $\text{Fe}^{\text{II}}-\text{NO}$ complexes of protein (5 μM heme final concentration), diluted in anaerobic 50 mM TEA, 50 mM NaCl, pH 7.5 buffer, were rapidly mixed with a saturated CO and 30 mM (final concentration) dithionite trap^{30,31} in the same buffer (anaerobic). Data were acquired by scanning periodically on a Cary 3E spectrophotometer equipped with a Neslab RTE-100 constant-temperature bath set to 20 $^{\circ}\text{C}$. The dissociation of NO from the heme was monitored as the formation of the $\text{Fe}^{\text{II}}-\text{CO}$ complex at 424 nm. Difference spectra were calculated by subtracting the first scan from each subsequent scan. The NO dissociation rate was determined from the increase in absorbance at 424 nm versus time and fit with a single exponential. Each experiment was done a minimum of six times, and the resulting rates were averaged. The dissociation rates measured are independent of dithionite concentration (300, 30 and 3 mM dithionite were tested).

Accession codes. GenBank identifiers: bovine $\beta 1$, P16068; *Drosophila* $\beta 1$, NP_524603; *Rattus* $\beta 1$, NP_036901; human $\beta 1$, AAB94877; *Nostoc*, ZP_00111432; *Vibrio*, NP_233107; *Shewanella*, NP_717745; *Caulobacter*, NP_421786; *Legionella*, AAU28519; *Thermoanaerobacter*, NP_622340; *Clostridium*, NO_349837; *Desulfovibrio*, ZP_00131180. Protein Data Bank identifiers: structures of Tt H-NOX, 1U55, 1U56 and 1U4H. BIND (<http://bind.ca/>) identifier: 261912.

ACKNOWLEDGMENTS

The Laboratory Directed Research and Development (LDRD) Fund from Lawrence Berkeley National Lab provided funding to M.A.M., the US National Science Foundation to S.H.H. and the Ruth L. Kirschstein National Research Service Award to E.M.B. (F32GM069302). We very gratefully acknowledge W. Belliston-Bittner, B. Leigh, J. Winkler and H. Gray at the Beckman Institute Laser Resource Center at the California Institute of Technology for their essential help in measuring oxygen association rates. We also thank J.H. Davis, P. Pellicena and J. Kuriyan at the University of California, Berkeley, as well as J. Dixon at the University of California, San Diego, and D. Ballou at the University of Michigan for helpful discussions.

COMPETING INTERESTS STATEMENT

The authors declare that they have no competing financial interests.

Received 28 February; accepted 15 April 2005

Published online at <http://www.nature.com/nchembio>

- Denninger, J.W. & Marletta, M.A. Guanylate cyclase and the NO/cGMP signaling pathway. *Acta Biochem. Biophys.* **1411**, 334–350 (1999).
- Iyer, L.M., Anantharaman, V. & Aravind, L. Ancient conserved domains shared by animal soluble guanylyl cyclases and bacterial signaling proteins. *BMC Genomics* **4**, 5 (2003).

- Karow, D.S. *et al.* Spectroscopic characterization of the soluble guanylate cyclase-like heme domains from *Vibrio cholerae* and *Thermoanaerobacter tengcongensis*. *Biochemistry* **43**, 10203–10211 (2004).
- Pellicena, P. *et al.* Crystal structure of an oxygen-binding heme domain related to soluble guanylate cyclases. *Proc. Natl. Acad. Sci. USA* **101**, 12854–12859 (2004).
- Mathews, A.J. & Olson, J.S. Assignment of rate constants for O_2 and CO binding to α -subunit and β -subunit within R-state and T-state human hemoglobin. *Methods Enzymol.* **232**, 363–386 (1994).
- Draghi, F. *et al.* Controlling ligand binding in myoglobin by mutagenesis. *J. Biol. Chem.* **277**, 7509–7519 (2002).
- Olson, J.S. & Phillips, G.N. Kinetic pathways and barriers for ligand binding to myoglobin. *J. Biol. Chem.* **271**, 17593–17596 (1996).
- Springer, B.A., Sligar, S.G., Olson, J.S. & Phillips, G.N. Mechanisms of ligand recognition in myoglobin. *Chem. Rev.* **94**, 699–714 (1994).
- Aono, S. *et al.* Resonance Raman and ligand binding studies of the oxygen-sensing signal transducer protein HemAT from *Bacillus subtilis*. *J. Biol. Chem.* **277**, 13528–13538 (2002).
- Kundu, S., Trent, J.T. & Hargrove, M.S. Plants, humans and hemoglobins. *Trends Plant Sci.* **8**, 387–393 (2003).
- Wittenberg, J.B., Bolognesi, M., Wittenberg, B.A. & Guertin, M. Truncated hemoglobins: a new family of hemoglobins widely distributed in bacteria, unicellular eukaryotes, and plants. *J. Biol. Chem.* **277**, 871–874 (2002).
- Deinum, G., Stone, J.R., Babcock, G.T. & Marletta, M.A. Binding of nitric oxide and carbon monoxide to soluble guanylate cyclase as observed with resonance raman spectroscopy. *Biochemistry* **35**, 1540–1547 (1996).
- Oertling, W.A., Kean, R.T., Wever, R. & Babcock, G.T. Factors affecting the iron oxygen vibrations of ferrous oxy and ferryl oxo heme-proteins and model compounds. *Inorg. Chem.* **29**, 2633–2645 (1990).
- Phillips, G.N. *et al.* Bound CO is a molecular probe of electrostatic potential in the distal pocket of myoglobin. *J. Phys. Chem. B* **103**, 8817–8829 (1999).
- Nioche, P. *et al.* Femtomolar sensitivity of a NO sensor from *Clostridium botulinum*. *Science* **306**, 1550–1553 (2004).
- Zhao, Y., Brandish, P.E., Ballou, D.P. & Marletta, M.A. A molecular basis for nitric oxide sensing by soluble guanylate cyclase. *Proc. Natl. Acad. Sci. USA* **96**, 14753–14758 (1999).
- Gray, J.M. *et al.* Oxygen sensation and social feeding mediated by a *C. elegans* guanylate cyclase homologue. *Nature* **430**, 317–322 (2004).
- Morton, D.B. Atypical soluble guanylyl cyclases in *Drosophila* can function as molecular oxygen sensors. *J. Biol. Chem.* **279**, 50651–50653 (2004).
- Quillin, M.L. *et al.* Structural and functional effects of apolar mutations of the distal valine in myoglobin. *J. Mol. Biol.* **245**, 416–436 (1995).
- Hvitved, A.N., Trent, J.T., Premer, S.A. & Hargrove, M.S. Ligand binding and hexacoordination in *Synechocystis* hemoglobin. *J. Biol. Chem.* **276**, 34714–34721 (2001).
- Hargrove, M.S. *et al.* Crystal structure of a nonsymbiotic plant hemoglobin. *Structure Fold Des.* **8**, 1005–1014 (2000).
- Pesce, A. *et al.* Human brain neuroglobin structure reveals a distinct mode of controlling oxygen affinity. *Structure* **11**, 1087–1095 (2003).
- Gong, W., Hao, B. & Chan, M.K. New mechanistic insights from structural studies of the oxygen-sensing domain of *Bradyrhizobium japonicum* FixL. *Biochemistry* **39**, 3955–3962 (2000).
- Gibson, Q.H. & Smith, M.H. Rates of reaction of *Ascaris* haemoglobins with ligands. *Proc. R. Soc. Lond. Biol.* **163**, 206–214 (1965).
- Hargrove, M.S. *et al.* Characterization of recombinant soybean leghemoglobin and apolar distal histidine mutants. *J. Mol. Biol.* **266**, 1032–1042 (1997).
- Kiger, L. *et al.* Trematode hemoglobins show exceptionally high oxygen affinity. *Biophys. J.* **75**, 990–998 (1998).
- Gilles-Gonzalez, M.A. *et al.* Heme-based sensors, exemplified by the kinase FixL, are a new class of heme protein with distinctive ligand binding and autoxidation. *Biochemistry* **33**, 8067–8073 (1994).
- Chang, A.L. *et al.* Phosphodiesterase A1, a regulator of cellulose synthesis in *Acetobacter xylinum*, is a heme-based sensor. *Biochemistry* **40**, 3420–3426 (2001).
- Dmochowski, I.J., Winkler, J.R. & Gray, H.B. Enantiomeric discrimination of Ru-substrates by cytochrome P450cam. *J. Inorg. Biochem.* **81**, 221–228 (2000).
- Moore, E.G. & Gibson, Q.H. Cooperativity in the dissociation of nitric oxide from hemoglobin. *J. Biol. Chem.* **251**, 2788–2794 (1976).
- Kharitonov, V.G., Sharma, V.S., Magde, D. & Koesling, D. Kinetics of nitric oxide dissociation from five- and six-coordinate nitrosyl hemes and heme proteins, including soluble guanylate cyclase. *Biochemistry* **36**, 6814–6818 (1997).